ARCHIVES OF ELECTRICAL ENGINEERING VOL. 69(1), pp. 101–116 (2020)

DOI 10.24425/aee.2020.131761

Sensorless backstepping control using a Luenberger observer for double-star induction motor

HADJI CHAABANE [1], KHODJA DJALAL EDDINE [1,2], CHAKROUNE SALIM [1]

[1] *Research Laboratory of Electrical Engeneering, University of M'sila*
BP 166, Ichbilia 28000, Algeria
e-mails: {chaabane.hadji/djalaleddine.khodja/salim.chakroun}@univ-msila.dz

[2] *Signals & Systems Laboratory, Institute of Electrical and Electronic Engineering*
Boumerdes, Algeria

(Received: 22.05.2019, revised: 24.09.2019)

Abstract: In this paper, we propose sensorless backstepping control of a double-star induction machine (DSIM). First, the backstepping approach is designed to steer the flux and speed variables to their references and to compensate uncertainties. Lyapunov"s theory is used and it demonstrates that the dynamic tracking of trajectories tracking is asymptotically stable. Second, unfortunately, this law control called sophisticated is a major problem which leads to the necessity of using a mechanical sensor (speed, load torque). This imposes an additional cost and increases the complexity of the montage. In practice, this variable is unknown and its measurement is expensive. To restrain this problem we estimate speed and load torque by using a Luenberger observer (LO). Simulation results are provided to illustrate the performance of the proposed approach in high and low variable speeds and load torque disturbance.

Key words: backstepping control, double star induction machine (DSIM) drive, Luenberger observer

1. Introduction

The growth of electrical energy consumption and high-power electrical applications, such as rail traction or marine propulsion, have led to the use of polyphase machines (whose number of phases is greater than three) to segment the power. Polyphase machines offer an interesting alternative to reducing stress on switches and windings. Indeed, the multiplication of the number of phases allows for splitting of the power and thus reduction of the switched voltages with a given current. In addition, these machines can reduce the amplitude and increase the frequency of torque ripple allowing the mechanical load to filter more easily. Thus, the multiplication of the number of phases offers high reliability by making it possible to operate with one or more faulty phases. However, the dynamic structure is strongly nonlinear and the existence of strong coupling between the torque and the flux creates a difficulty of control [1]. Among the most common machines of multiphase machines is the Asynchronous Machine Double Star (DSIM). In the conventional configuration, two identical three-phase windings constituting the two stars share the same stator and are shifted by an electric angle. They have the same number of poles and are powered at the same frequency. The structure of the rotor remains identical to that of a three-phase machine, so it can be either squirrel cage or wound to form a three-phase winding. Such a machine has the advantage, besides the power segmentation and the interesting redundancy that it introduces, it significantly reduces the electromagnetic torque ripple and the rotor losses [2].

Modern control techniques lead to the control of asynchronous machines comparable to that of the DC machine. These techniques include direct torque control, state feedback control, vector control, and adaptive control. These techniques use both conventional and modern regulators that make the aforementioned controls robust.

The sliding mode control presented in [2] was used for the variable speed drive of the dual star asynchronous machine. The control thus constructed makes it possible to ensure, in addition to well tracking performance, a fast dynamic and a short response time. However, this control law represents some major disadvantage related to the use of the switching function in the control law to ensure the passage of the approach phase of the slip. This gives rise to the phenomenon of chatter which consists of abrupt and rapid variations of the control signal.

Adaptive control which is more robust has been used in [3, 4] as a proposed solution to the problem of trajectory tracking and browsing phenomenon as well as mainly for the adaptation of the gains of the fuzzy or neural regulator.

The fuzzy regulator has been proposed in [4, 5], for the adjustment of the sliding surface of a regulator by sliding mode which guarantees to give a certain robustness. The results obtained in simulation show that the performance is much better than that obtained with a sliding mode. Fuzzy logic has been a real success in the control of dual star asynchronous machines [5, 6].

The DTC control is less sensitive to parametric variations of the machine and allows one to obtain a precise and fast torque dynamics [7]. In most of these new strategies, hysteresis comparators are discarded and replaced by new controllers (microprocessor, microcontroller, DSP). These strategies have been proposed in order to improve the performance of the conventional control and to allow the control of the switching frequency of the inverter.

The regulation of the speed of induction motors by Neural Networks control presented in [8], is to improve the signal quality of the speed (band width smaller) and to reject the disturbance (load torque). However, this robustness decreases if the parametric variations are very important.

On the other hand the combination of these approaches as neuro-fuzzy at [8], adaptive blur at [4, 9], adaptive with DTC at [7] and the ANFIS controller (Adaptive Network Fuzzy Inference System) in [8] gives better results in performance, robustness, pursuit and stability. It also helps to achieve a better response time.

In fact, it can be concluded that each type of control can be advantageous when used in one direction and disadvantageous when used in another, because of its dynamic structure (DSIM) is strongly non-linear and coupled. The situation changes with the appearance of the theory of nonlinear systems in control theory where the researchers are interested in new control techniques that allow for approaching large systems with a systematic approach. Among these methods is the backstepping control method, which was introduced during the 1990s by several researchers, Kokotovic is quoted. The application of the latter is found, for example, in the field of aeronautics in [10], and in the field of robotics in [10, 11], and electrical machines [12, 13], and also for power network power regulation in [14].

The coupling between the backstepping approach and sliding mode control in [10], and use of the neural network for induction motors in [15, 16], have given some satisfactory results by ensuring the system convergence (stability) even if the settling time considered is a little bit longer and is not practical in implementation (complex) [17, 18].

The majority of the control laws of asynchronous machines such as vector and non-linear commands require the measurement not only of the stator currents (possibly stator voltages) but also of the mechanical speed. Moreover, the load torque is a measurable disturbance but the price of the sensor often makes this measurement unrealistic. The control without the mechanical sensor (speed, load torque) has become a major concern in the industry.

Among several approaches without mechanical sensor of the asynchronous machine used neural networks [15, 16]. Another approach is based on a model of behavior of the machine which is based on observation techniques from the automatic extended Kalman filters in [17], extended Luenberger filters in [17, 18], adaptive methods in [19], and non-linear observers such as, for example, second order sliding mode observers [20].

All the traditional approaches to speed sensorless vector control use the method of flux and slip estimation using stator currents and voltages but that speed estimations are erroneous, particularly the ones related to the low-speed range. MRAS (Model Reference Adaptive System) techniques are also used to estimate the speed of an induction motor [21]. These also show speed errors in the low-speed range and settle to an incorrect steady-state value. The extended Kalman filter has been used for the speed sensorless vector control of an induction motor, but it remains the most sensitive since it requires the exact values of the machine parameters [22].

This paper is organized as follows: the field - oriented dual star induction motor (DSIM) is described in Section 2, Section 3 reviews the backstepping control design, in Section 4 the estimation of the rotor speed and load torque using a developed Luenberger observer is discussed (using only electrical measurements). Finally, the simulation results and conclusion are given in Section 5.

2. Backstepping control of the dual stator asynchronous motor

The difficulty in controlling a dual stator asynchronous machine lies in the fact that there is strong coupling between the input and output variables and the internal variables of the machine such as flux, torque and speed. The types of controls as conventional control methods such as torque control by frequency slip and the flux ratio of voltage to frequency, cannot ensure significant dynamic performance. The development of electronics at current level, in the use of static and semi-conductive converters, has allowed the application of new control algorithms such as the vector control (identical to a DC machine with separated excitation) which is based on the decoupling of flux and torque in AC machines. The principle of the vector control called control by flux orientation, obtained by the adjustment of torque by a component of the current and the flux by the other component, that is to say orients another of the stator flux components, rotor or the gap on a reference axis rotating at the rotating field speed. The vector control leads to high industrial performance of asynchronous drives. If we make the rotor flux coincide with the axis (d) of the frame linked to the rotating field and after the rotor flux orientation by:

$$\Phi_{rd} = \Phi_{rd}, \qquad \Phi_{rd} = 0, \tag{1}$$

where the instantaneous value of the electromagnetic torque is given by:

$$C_{em} = p\frac{L_m}{L_m + L_r}\left(I_{qs1} + I_{qs2}\right)\Phi_r. \tag{2}$$

So the main objective after [17, 18] is to produce reference voltages for the static voltage converters supplying the (DSIM). Note that X^* for reference represents the desired reference trajectories for X (torque, flux, voltages and currents). Applying the orientation of the rotor flux on the equations system of the machine leads to the equation [1, 18] with:
ω^*_{sr}, which is the slip angular frequency; $T_r = \dfrac{L_r}{R_r}$ which denotes the rotor time constant and $\omega^*_s = \omega^*_{sr} + \omega_r$, the final expressions of the slip speed are:

$$\omega^*_{sr} = \frac{R_r L_m}{L_m + L_r}\left(I^*_{qs1} + I^*_{qs2}\right). \tag{3}$$

Consequently, the electrical and mechanical equations for the system after these transformations in the space control may be written as follows:

$$\frac{\mathrm{d}}{\mathrm{d}t}I_{ds1} = \frac{1}{L_{s1}}\left[V_{ds1} - R_{s1}I_{ds1} + \omega^*_s\left(L_{s1}I_{qs1} + T_r\Phi^*_r\omega^*_{sr}\right)\right], \tag{4}$$

$$\frac{\mathrm{d}}{\mathrm{d}t}I_{qs1} = \frac{1}{L_{s1}}\left[V_{qs1} - R_{s1}I_{qs1} - \omega^*_s\left(L_{s1}I_{ds1} + \Phi^*_r\right)\right], \tag{5}$$

$$\frac{\mathrm{d}}{\mathrm{d}t}I_{ds2} = \frac{1}{L_{s1}}\left[V_{ds2} - R_{s2}I_{ds2} + \omega^*_s\left(L_{s2}I_{qs2} + T_r\Phi^*_r\omega^*_{sr}\right)\right], \tag{6}$$

$$\frac{\mathrm{d}}{\mathrm{d}t}I_{qs2} = \frac{1}{L_{s1}}\left[V_{qs2} - R_{s2}I_{qs2} - \omega^*_s\left(L_{s2}I_{ds2} + \Phi^*_r\right)\right], \tag{7}$$

$$\frac{\mathrm{d}}{\mathrm{d}t}\Omega = \frac{1}{J}\left[pc_1\left(I_{qs1} + I_{qs2}\right)\Phi^*_r - K_f\Omega - C_r\right], \tag{8}$$

$$\frac{\mathrm{d}}{\mathrm{d}t}\Phi_r = -c_2\Phi_r + R_r c_1\left(I_{ds1} + I_{ds2}\right), \tag{9}$$

where the factors: c_1, c_2 are given by

$$c_1 = \frac{L_m}{L_m + L_r} \quad \text{and} \quad c_2 = \frac{R_r}{L_m + L_r}.$$

R_r is the rotor resistance; $R_{s1,2}$ is stator's 1 and 2 resistance; L_m represents the mutual inductances; $L_{s1,2}$ is stator's 1, and 2 self-inductances; J is the moment of inertia; K_f is the viscous friction coefficient; P represents the pole-pair number; L_r is the rotor self-inductance.

The rotor flux are estimated by the following two equations: (with the sign (ˆ) that represents the estimated value either by the estimator or the observer):

$$\frac{\mathrm{d}}{\mathrm{d}t}\hat{\Phi}_{dr} = R_r c_1 \left(I_{ds1} + I_{ds2}\right) + \omega_{sr}^* \hat{\Phi}_q + c_2 \hat{\Phi}_{dr}\,, \tag{10}$$

$$\frac{\mathrm{d}}{\mathrm{d}t}\hat{\Phi}_{qr} = R_r c_1 \left(I_{qs1} + I_{qs2}\right) + \omega_{sr}^* \hat{\Phi}_{dr} + c_2 \hat{\Phi}_{qr}\,. \tag{11}$$

The rotor fluxes module is calculated as follows:

$$\hat{\Phi}_r = \sqrt{\hat{\Phi}_{dr}^2 + \hat{\Phi}_{qr}^2}\,. \tag{12}$$

3. The step of backstepping control

The backstepping control technique provides a systematic method for designing a controller for nonlinear systems [19]. The idea is to compute a control law in order to guarantee stability based on Lyapunov's theory.

The method consists in breaking up the system into a set of decreasing nested subsystems. The calculation of the Lyapunov function is then performed recursively from the inside of the loop. The objective of this technique is to calculate, at each stage of the process, a virtual command which is thus generated to ensure the convergence of the system towards its equilibrium state [20]. This can be achieved from the functions of Lyapunov which ensure, step by step, the stabilization of each synthesis step. Unlike most other methods, backstepping has no nonlinearity constraints.

Lyapunov's theory is important for the stability of dynamical systems and the control theory, where this stability is based on choosing the Lyapunov candidate function $V(x) \prec 0$ (a positive scalar function) for the system state variables, then on choosing the law of control which will make this function $\dot{V}(x) \prec 0$, for all $x \neq 0$, and $\dot{V}(0) = 0$.

If the both conditions are verified ($V(x) \prec 0$, $\dot{V}(x) \prec 0$), the system is globally asymptotically stable, as: $t \to +\infty$ [16].

3.1. First step "speed loop, flux loop"

In this step, the objective is to force the rotation speed ω, to follow a given reference ω_{ref} as well as possible. The first error variable e_1 is defined as the error between the speed of rotation and the speed desired by:

$$e_1 = \omega_{\mathrm{ref}} - \hat{\omega}. \tag{13}$$

By derivation, we obtain: $\dot{e}_1 = \dot{\omega}_{\mathrm{ref}} - \dot{\hat{\omega}}$.

To ensure the operation of the machine in the linear regime (out of saturation), a flow control is also carried out such that Φ_r follows the imposed trajectory Φ_{ref}.

To achieve this goal we pose: $e_2 = \Phi_r^* - \hat{\Phi}_r$.

By derivation, we obtain: $\dot{e}_2 = \Phi_r^* - \dot{\hat{\Phi}}_r$.

The first Lyapunov candidate function is defined by:

$$V_1 = \frac{1}{2}\left(e_1^2 + e_2^2\right).$$

By derivation, we obtain:

$$\dot{V}_1 = e_1\dot{e}_1 + e_1\dot{e}_2 .$$

$$\dot{V}_1 = e_1\left[\omega_{\text{ref}} - \frac{1}{J}\left(pc_1\left(I_{qs1} + I_{qs2}\right)\Phi_r^* + K_f\omega + \hat{C}_r\right)\right] + e_2\left[\Phi_r^* + c_2\hat{\Phi}_r - R_r c_1\left(I_{ds1} + I_{ds2}\right)\right].$$

According to the Lyapunov stability, the origins $e_1 = 0$ and $e_2 = 0$ of the system are asymptotically stable when $\dot{V}_1$ is defined negative.

We then define $\left(I_{qs1} + I_{qs2}\right)$ and $\left(I_{ds1} + I_{ds2}\right)$ as the virtual control. Indeed, for an expert in the field of electrical machines, this choice of virtual control is normal, that is to say, one looks for the value that the virtual control must take so that the origin is stable, and the stabilizing virtual function is determined so that:

$$\dot{V}_1 = -K_1e_1^2 - K_2e_2^2 < 0 \quad \text{with} \quad K_1 < 0, \quad K_2 < 0.$$

We find:

$$I_{qs1}^* + I_{qs2}^* = \frac{J}{pc_1\Phi_{\text{ref}}}\left[\omega_{\text{ref}} + \frac{K_f}{J}\hat{\omega} + \frac{\hat{C}_r}{J} + K_1e_1\right]. \tag{14}$$

$$I_{ds1}^* + I_{ds2}^* = \frac{J}{c_1L_m}\left[c_2\hat{\Phi}_r + \Phi_r^* + K_2e_2\right], \tag{15}$$

where: $I_{qs1}^* + I_{qs2}^*$ and $I_{ds1}^* + I_{ds2}^*$, represent the references of the components of the current.

3.2. Second step "currents loop"

For this step, our goal is the elimination of the current regulators by the calculation of the control voltages. Other errors concerning the components of the stator current and their references are defined as:

$$e_3 = I_{qs1}^* - I_{qs1}, \quad e_4 = I_{ds1}^* - I_{ds1}, \quad e_5 = I_{qs2}^* - I_{qs2}, \quad e_6 = I_{ds2}^* - I_{ds2}.$$

The dynamics of errors is given by:

$$\dot{e}_3 = \dot{I}_{qs1}^* - \dot{I}_{qs1} = \dot{I}_{qs1}^* - \frac{1}{L_{s1}}\left(V_{qs1} + \gamma_1\right),$$

$$\dot{e}_4 = \dot{I}_{ds1}^* - \dot{I}_{ds1} = \dot{I}_{ds1}^* - \frac{1}{L_{s1}}\left(V_{ds1} + \gamma_2\right),$$

$$\dot{e}_5 = \dot{I}_{qs2}^* - \dot{I}_{qs2} = \dot{I}_{qs2}^* - \frac{1}{L_{s2}}\left(V_{qs2} + \gamma_3\right),$$

$$\dot{e}_6 = \dot{I}_{ds2}^* - \dot{I}_{ds2} = \dot{I}_{ds2}^* - \frac{1}{L_{s2}}\left(V_{ds2} + \gamma_4\right),$$

with:

$$\gamma_1 = -R_{s1}I_{qs1} - \omega_s^*\left(L_{s1}I_{ds1} + \Phi_r^*\right),$$

$$\gamma_2 = -R_{s1}I_{ds1} - \omega_s^*\left(L_{s1}I_{qs1} + T_r\Phi_r^*\omega_{sr}^*\right),$$

$$\gamma_3 = -R_{s2}I_{qs2} - \omega_s^* \left(L_{s2}I_{ds2} + \Phi_r^*\right),$$

$$\gamma_4 = -R_{s2}I_{ds2} - \omega_s^* \left(L_{s2}I_{qs2} + T_r\Phi_r^*\omega_{sr}^*\right).$$

The new function of Lyapunov is given by:

$$V_2 = \left(V_1 + e_3^2 + e_4^2 + e_5^2 + e_6^2\right),$$

$$\dot{V}_2 = V_1 + \left(-K_3e_3^2 - K_4e_4^2 - K_5e_5^2 + K_6e_6^2\right),$$

$$\dot{V}_2 = \left(\dot{V}_1 + e_3\dot{e}_3 + e_4\dot{e}_4 + e_5\dot{e}_5 + e_6\dot{e}_6\right).$$

We look for the value that must be taken by the reference control $\left(V_{ds1}^*, V_{qs1}^*, V_{ds2}^*, V_{dq2}^*\right)$ for the origin to be stable. The stabilizing virtual function is determined so that:

$$\dot{V}_2 = \dot{V}_1 + \left(-K_3e_3^2 - K_4e_4^2 - K_5e_5^2 + K_6e_6^2\right) < 0.$$

With K_3, K_4, K_5, K_6 being positive gains, the stator voltage can be rewritten as:

$$V_{qs1}^* = L_{s1}\left(K_3e_3 - \gamma_1 + \dot{I}_{qs1}^*\right), \tag{16}$$

$$V_{ds1}^* = L_{s1}\left(K_4e_4 - \gamma_2 + \dot{I}_{ds1}^*\right), \tag{17}$$

$$V_{qs2}^* = L_{s2}\left(K_5e_5 - \gamma_3 + \dot{I}_{qs2}^*\right), \tag{18}$$

$$V_{ds2}^* = L_{s2}\left(K_6e_6 - \gamma_4 + \dot{I}_{ds2}^*\right). \tag{19}$$

4. Proposed Luenberger observer developed for speed and load torque sensorless vector control

4.1. Equation of observer

The purpose of the observer is to provide at every moment the state vector value or aevaluation of it. In general, we consider that we always have system state equations. The trivial case consist in performing open loop implementation, as illustrated in Figure 1, and it is based on a model of the system, called the estimator, operating in an open loop. The complete structure of the observer includes a feedback loop to correct the error between the output of the system and that of the model.

By hypothesis, we suppose that the concerned observed system is completely observable and completely controllable. It is defined by the equation of state:

$$\begin{cases} \dot{X} = AX + Bu \\ y = CX + Du \end{cases}, \tag{20}$$

with:

$$X^T = [\vartheta \;\; x \;\; C_r], \quad A = \begin{bmatrix} 0 & 1 & 0 \\ 0 & a_1 & a_2 \\ 0 & 0 & 0 \end{bmatrix}, \quad B^T = [0 \;\; a_3 \;\; 0], \quad C = [1 \;\; 0 \;\; 0], \quad D = 0,$$

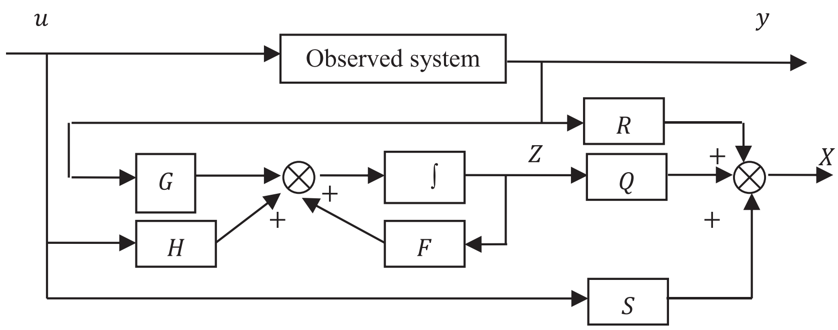

Fig. 1. Block diagram of the proposed Luenberger observer

$$u = \left(I_{qs1} + I_{qs2}\right), \quad a_1 = -\frac{K_f}{J}, \quad a_2 = -\frac{1}{J}, \quad a_2 = \frac{2L_m\Phi_r^*}{J\left(L_m + L_r\right)}.$$

The observer of Luenberger is defined as a dynamic system whose state vector is denoted by Z of the dimension $(l, 1)$ and whose inputs correspond, on the one hand, to the input u of the dimension $(m, 1)$ and the output y of the observing system of the dimension $(r, 1)$. The equations of the observer are:

$$\dot{Z} = FZ + Hu + Gy \quad \text{(to study error stability)}.$$

$$\hat{X} = QZ + Ry + Su \quad \text{(to estimate } X\text{)}.$$

We impose the relation: $Z = LX + \varepsilon$, where: $\varepsilon = X - \hat{X}$, the error of estimations and we want the output $\hat{X}$ to be equal to X. After a shortest transient possible, it comes as:

$$\dot{Z} = FLX + F\varepsilon + Hu + GCX + GDu.$$

On the other hand: $\dot{Z} = L\dot{X} + \varepsilon$ which leads to:

$$[LA - FL - GC]X + [LB - H - GD]u + \dot{\varepsilon} = F\varepsilon. \tag{21}$$

To guarantee the independence of the observed system state and the input, the conditions of Luenberger are satisfied:

$$\begin{cases} LA - FL - GC = 0 \\ LB - H - GD = 0 \end{cases}. \tag{22}$$

Then we obtain the state equation of the error: $\dot{\varepsilon} = F\varepsilon$.

The dynamic of the error does not depend of the input u. However, the error tends to zero, it is enough that F is stable. The matrix F can be chosen but must have stable modes faster than those of the steady state (the pole placement technique has been used), the output equation of the observer is written as:

$$\hat{X} = QZ + Ry + Su = [QL + RC]X + [RD + s]u.$$

To guarantee that the output $\hat{x}$ is equal to x in the steady state, it is necessary to impose two conditions:

$$\begin{cases} QA - GRC = I \\ RD - S = 0 \end{cases} . \tag{23}$$

4.2. Observer under noise measurement

In the case, where the output y is disturbed by the additive noise ξ we can see the behavior of the proposed observer as:

– Taking the basic equation of the system and adding ξ the output:

$$\begin{cases} \dot{X} = AX + Bu \\ y = CX + Du + \xi \end{cases} . \tag{24}$$

– The observer will be:

$$\begin{cases} \dot{Z} = F + Hu + Gy \\ \hat{X} = QZ + Ry + Su \end{cases} .$$

From the relation: $Z = XL + \varepsilon$, and taking into account additive noise on the output of the observed system, Equation (21) becomes:

$$[LA - FL - GC]X + [LB - H - GD]u + \dot{\varepsilon} = F\varepsilon + G\xi. \tag{25}$$

Taking into account the conditions of Luenberger, it comes to:

$$\dot{\varepsilon} = F\varepsilon + G\xi\,.$$

So with the presence of noise the error of estimations can't be equal to zero, which decreases the performance of the observer. It is even possible to filter the output in order to eliminate the noise, but this filter can also eliminate its own information of the dynamic of the system.

5. Simulation and interpretation of results

A series of simulation tests were carried out on the backstepping approach of a (DSIM) drive, based on a Luenberger observer. Simulations have been realized under the Matlab environment. The parameters of the used of dual-star induction motor are indicated in Table 2. See Figure 2, the results presented in this article were made with the following synthesis parameters: the desired flux is fixed at $\Phi_r^* = 1\ Wb$ and $K_1 = K_2 = 500$, $K_4 = 300$, $K_5 = K_6 = 200$.

The output directly supplies the first component of the state system vector $y = \vartheta$ (estimated), and the matrix C of dimension $(1, 3)$. We deduce successively: L is the dimension $(2, 3)$, the state vector of the observer is of dimension 2, F is the matrix of dimension $(2, 3)$ and the matrices G, H, Q, R are, respectively, of dimensions $(2, 1)$, $(2, 1)$, $(3, 2)$, $(3, 1)$.

To facilitate, we can write F in the following observable form:

$$F = \begin{bmatrix} -f_1 & 1 \\ -f_0 & 0 \end{bmatrix}.$$

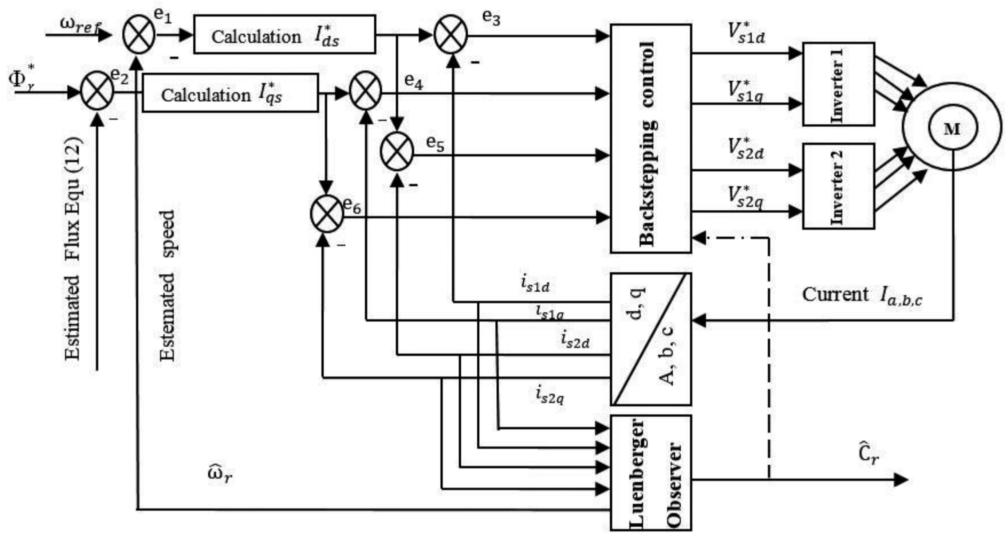

Fig. 2. General structure of the order by backstepping control with Luenberger observer of the (DSIM)

From the equation's solution $\det(\lambda I - F) = 0$, the characteristic equation of the observer is written as:

$$\lambda^2 + f_1\lambda + f_0 = 0.$$

The matrix A can be calculated in the point $(s = \lambda)$ by the solution of the equation: $\det(\lambda I - F) = 0$, this way we obtain: $\lambda = 0.01$ (s: derives Laplace).

We can chose -305, -70, for F matrix (choosing self-mode faster than modes of A (system)), so that:

$$(\lambda + 305)(\lambda + 70) = \lambda^2 + f_1\lambda + f_0.$$

We obtain: $f_1 = 375$, $f_0 = 21\,350$.

The observer equations are:

$$\dot{Z} = \begin{bmatrix} -f_1 & 1 \\ -f_0 & 0 \end{bmatrix} Z + \begin{bmatrix} h_1 \\ h_2 \end{bmatrix} \left(I_{qs1} + I_{qa2}\right) + \begin{bmatrix} g_1 \\ g_2 \end{bmatrix} y$$

and

$$\begin{bmatrix} \hat{\vartheta} l \\ \hat{\omega} \\ \hat{C}_r \end{bmatrix} = \begin{bmatrix} a & b \\ c & d \\ e & f \end{bmatrix} Z + \begin{bmatrix} r_1 \\ r_2 \\ r_3 \end{bmatrix} y.$$

Since the matrix D is zero, we deduce directly that S is equal to zero.

From the relation: $Z = LX + \varepsilon$ we can choose the matrix L in the following form:

$$L = \begin{bmatrix} L_0 & 1 & L_2 \\ L_1 & L_3 & 1 \end{bmatrix}.$$

Solving the Luenberger equation leads to

$$L_2 = \frac{1 - a_1}{f_1}, \quad L_3 = \frac{-f_0 L_0}{a_2}, \quad L_0 = L_3 - a_1 - f_1,$$

$$g_0 = f_1 L_0 - L_1, \quad g_1 = f_0 L_0,$$

$$H = LB = \begin{bmatrix} a_3 \\ a_3 L_3 \end{bmatrix} [QR] = \begin{bmatrix} L \\ C \end{bmatrix}^{-1}.$$

The first two columns correspond to Q and the last column to R.

Thus, the no-load start-up of the (DSIM) is performed and then the load torque step of $C_r = 14$ Nm is applied at a time of $t = 1{-}2.5$ s. At $t = 2.5$ s the load is eliminated. The speed reference is 250 rad/s until the time $t = 4$ s.

Figure 3 shows the actual and observed velocity curves. We note that the speed follows its reference. For the curve of the load torque, it is noted that the observation error is greater at the start-up since there are friction forces. However, the observer quickly converges, the electromagnetic torque achieves a significant peak at the startup and also the components of the current I_{qs}, see Figure 5, the signals follow their references and finally in Figure 4 the shape of the components of the rotor flux shows that the decoupling still maintains.

The results obtained for the application of the backstepping command by the Luenberger observer, show a clear improvement in performance, especially to the point where the load value

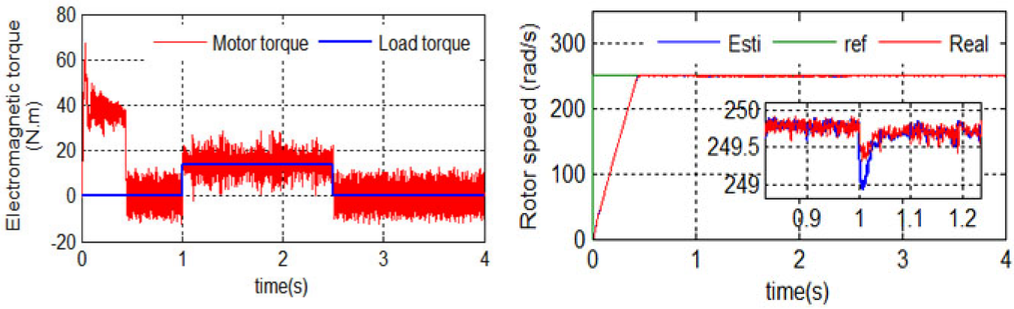

Fig. 3. Speed and torques responses using Luenberger observer

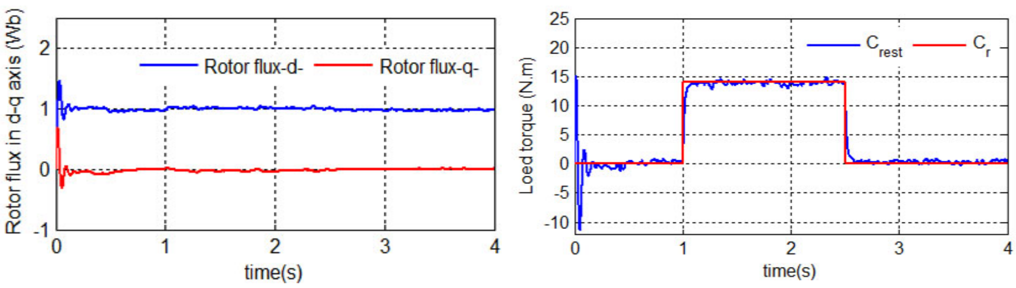

Fig. 4. Load torque and rotor flux responses using Luenberger observer

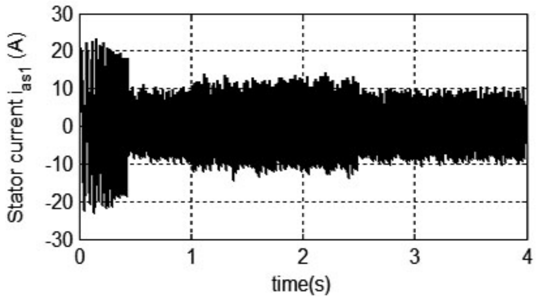

Fig. 5. Stator current responses using Luenberger observer

that was used by the control is unmeasured (unobserved). This improvement is reflected in the quality of the speed signal, as well as in the almost total rejection of the disturbance (load torque).

5.1. Robustness test

5.1.1. Robustness of the observer for low speed

In order to evaluate the performance of the observer, especially when the machine (DSIM) works in low speed, we have:

In the start stage, the load torque is maintained at zero, the speed of the machine reaches 20 rad/s and is held constant still when $t = 3$ s. So the load is applied between 1.5 s and 2.5 s. This first stage allows one to test and evaluate the performance and the robustness of the observer in low speed and nominal load (14 Nm).

At $t = 2$ s the machine accelerates steadily to achieve 200 rad/s), then at $t = 3.5$ s, we set the load to zero. This second stage is to test the behavior the machine (DSIM) during a big transition of speed, and robustness in high speed. Then we quickly decelerate the machine to 30 rad/at $t = 4$ s and maintain it steady at $t = 6$ s.

The obtained results show two terms:

In the term of trajectory following: the machine speed in Figure 6 follows correctly its reference speed. It shows only a small static gap during the startup. The same conclusion is reached for the load torque estimated in Figure 7.

In the term of noise rejection: the torque is well rejected, especially in low speed. Otherwise, a small gap appears during the law speed of the loaded machine (Figure 6: between 1.5 and 3.5 s).

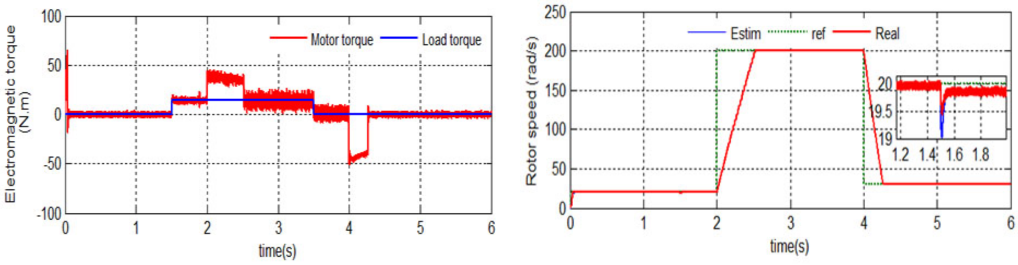

Fig. 6. Speed and torque responses of the machine with application at the backstepping command during low speed

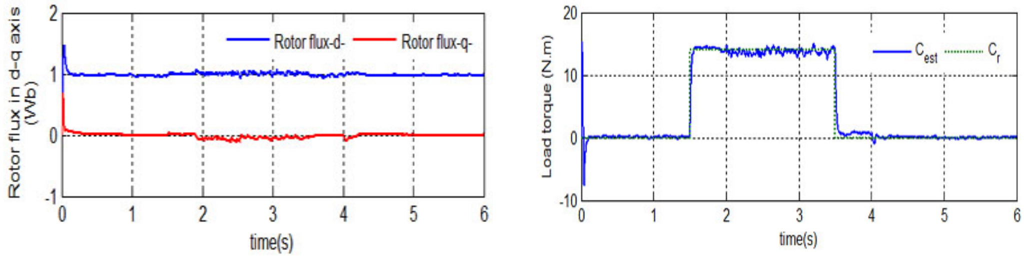

Fig. 7. Load torques and rotor flux responses of the machine at the application of the backstepping command during low speed

5.1.2. Robustness with respect to the variation rotor resistance

We study the robustness of the backstepping control based on a Luenberger observer opposite to the variation of the rotor parameters of the engine. The analysis of the robustness of control is explored as opposed to the variation of resistance the R_r of the engine according to the robustness tests presented in Figure 8. We note the insensitivity of the backstepping control with the Luenberger observer facing the variation of the rotor resistance R_r of the dual star asynchronous machine.

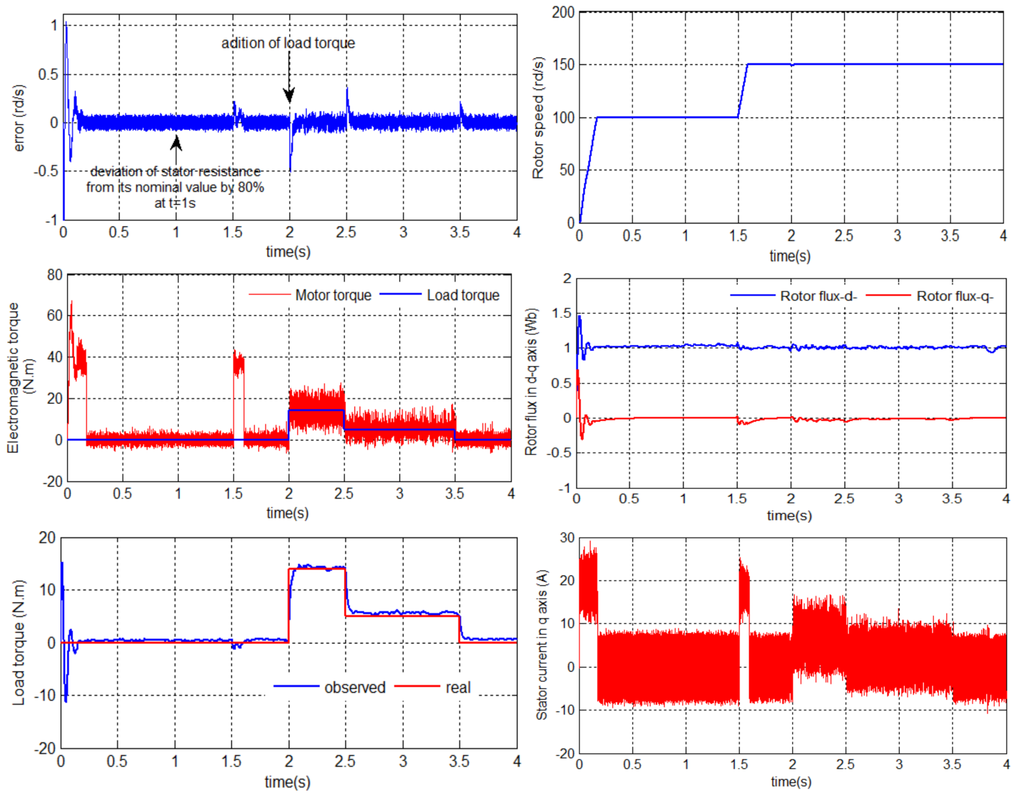

Fig. 8. Dynamic response of the machine with the application of the backstepping command during robustness tests with respect to rotor resistance R_r

6. Conclusion

In this paper, we used the backstepping recursive command with a Luenberger observer of the speed and torque resistance for the control of a dual-star asynchronous machine. It can clearly be seen that the development of the proposed robust control law has been applied. To avoid the problem of the persecutory effects of speed sensors and the resistant torque, a developed Luenberger observer has been proposed. The results obtained in simulation are very close to those obtained using a speed sensor, and as a perspective, it would be interesting to add an estimator for the rotor resistance, and developing the observer under noise.

Appendix 1

Table 1. Nomenclature of the parameters DSIM model

DSIM	Double-star induction motor
IFOC	Indirect field-oriented control
DFOC	Direct field-oriented control
PI	Proportional and integral
MRAC	Model reference adaptive control
FLC	Fuzzy logic controller
DTC	Direct Torque Control
DSP	Digital Signal Processor
LO	Luenberger observer
ANFIS	Adaptive Network Fuzzy Inference System
V_{ds}, V_{qs}, V_{dr}, V_{gr}	Stator and rotor voltages $d{-}q$ axis components
I_{ds}, I_{qs}, I_{dr}, I_{gr}, I_{qr}	Stator and rotor currents $d{-}q$ axis components
Φ_d, Φ_r, Φ_s	Stator-rotor flux
Φ_d, Φ_q	Stator flux $d{-}q$ axis components
ω_s, ω_r, ω_{sr}^*	Stator and rotor pulsation respectively and speed sleep reference
Φ_r^*	Rotor flux control reference
R_s, R_r	Stator-rotor resistance
C_r	Load torque
ω	Mechanical speed
C_{em}	Electromagnetic torque
L_s, L_r, L_m	Stator- and rotor inductance, mutual inductance respectively
J	Total inertia
P	Number of pole pairs
K_f	Friction coefficient
ϑ_s	Angle between stator and rotor flux

Appendix 2

Table 2. Machine parameters

Parameter name	Symbol	Value	Unit
Stator resistances	$R_{s1} = R_{s2} = R_s$	3.72	Ω
Rotor resistance	R_r	3.72	Ω
Stator self-inductances	$L_s = L_{s1} = L_{s2}$	0.022	H
Rotor self-inductance	L_r	0.006	H
Mutual inductance	L_m	0.3672	H
Moment of inertia	J	0.0662	Kg·m^2
Viscous friction coefficient	K_f	0.001	N·m/rad
Supply frequency	f	50	Hz
Pole pairs number	p	1	/

References

[1] Drozdowski P., *Speed control of multiphase cage induction motors incorporating supply sequence*, Archives of Electrical Engineering, vol. 63, no. 4, pp. 511–534 (2014).

[2] Amimeur H., Abdessemed R., *A Sliding Mode Control Associated to the Field Oriented Control of Dual Stator Induction Motor Drives*, Revue des Energies Renouvelables, vol. 11, no. 2, pp. 317−327 (2008).

[3] Fischle K., Schroder D., *An improved stable adaptive fuzzy control method*, IEEE transactions on fuzzy systems, vol. 7, no. 1, pp. 27–40 (1999).

[4] Saghafinia A., Wooi P.H., *Adaptive fuzzy sliding mode control into chattering free IM drive*, IEEE Transactions on Industry Applications, vol. 51, no. 1, pp. 692–701 (2015).

[5] Tir Z., Youcef S., *Fuzzy logic field oriented control of double star induction motor drive*, Electrical Engineering, vol. 99, no. 2, pp. 495–503 (2017).

[6] Youb L., Sebti B., *Design of an adaptive fuzzy control system for dual star induction motor drive*, Advances in Electrical and Computer Engineering, vol. 18, no. 3, pp. 37–44 (2018).

[7] Akkari N., Chaghi A., *Speed control of doubly star induction motor using direct torque DTC based to on model reference adaptive control (MRAC)*, International Journal of Hybrid Information Technology, vol. 7, no. 2, pp. 19–28 (2014).

[8] Brandstetter P., *Sensorless control of DC drive using artificial neural network*, Acta Polytechnica Hungarica, vol. 11, no. 10, pp. 5–20 (2014).

[9] Ashfaq M., Wang D., *Modeling and backstepping based nonlinear control strategy for a 6 DOF quadrotor helicopte*r, Chinese Journal of Aeronautics, vol. 21, no. 3, pp. 261–268 (2008).

[10] Bouadi H., Bouchoucha M., *Sliding mode control based on backstepping approach for an UAV type quadrotor*, International Journal of Mechanical, Aerospace, Industrial, vol. 1, no. 2, pp. 39–44 (2007).

[11] Horch M., Boumediene A., *Nonlinear integral backstepping control for induction motor drive with adaptive speed observer using super twisting strategy*, Electrotehnică, electronică, automatică, vol. 64, no. 1, pp. 24–32 (2015).

[12] Chaouch S., *Backstepping control design of sensorless speed induction motor based on MRAS technique*, International Review of Electrical Engineering, vol. 2, no. 1, pp. 738–744 (2007).

[13] Benakcha M., Benalia L., *Backstepping control of dual stator induction generator used in wind energy conversion system*, International Journal of Renewable Energy Research, vol. 8, no. 1, pp. 385–395 (2018).

[14] Hadiouche D., Razik H., *Study and simulation of space vector PWM control of double star induction motors*, 7th IEEE International Power Electronics Congress, Technical Proceedings, Acapulco, Mexico, pp. 42–47 (2000).

[15] Sadouni R., Meroufel A., *Performances comparative study of field oriented control (FOC) and direct torque control (DTC) of dual three phase induction motor*, International Journal Of Circuits, Systems and Signal Processing, vol. 6, no. 2, pp. 163–170 (2012).

[16] Mohamed H., Boumediene A., Baghli L., *Nonlinear integral backstepping control for induction motor drive with adaptive speed observer using super twisting strategy*, Electrotehnica, Electronica, Automatica, vol. 64, no. 1, pp. 24–32 (2016).

[17] Laoufi A., Hazzab A., *Direct field oriented control using backstepping technique for induction motor speed control*, International Journal of Applied Engineering Research, vol. 1, no. 1, pp. 37−50 (2006).

[18] Zaafouri A., Ben Regaya C., Chaari A ., *Backstepping approach applied for control and on-line adaptation of the rotor resistance*, World Applied Sciences Journal, vol. 28, no. 8, pp. 1120–1126 (2013).

[19] Theocharis J., Petridis V., *Neural network observer for induction motor control*, IEEE Control Systems Magazine, vol. 14, no. 2, pp. 26–37 (1994).

[20] Mabrouk J., Kamel J., Yassine K., *A luenberger state observer for simultaneous estimation of speed and rotor resistance in sensorless indirect stator flux orientation control of induction motor drive*, IJCSI International Journal of Computer Science, vol. 8, no. 6, pp. 116–125 (2011).

[21] Jie Y., Wencen W., *An adaptive luenberger observer for speed sensorless estimation of induction machines*, Annual American Control Conference (ACC), Milwaukee, WI, USA, pp. 307–312 (2018).

[22] Davila J., Fridman L., *Second-order sliding-mode observer for mechanical systems*, IEEE Transactions on Automatic Control, vol. 50, no. 11, 1785–1789 (2005).